Steady Finite-Amplitude Rayleigh–Bénard Convection in Nanoliquids Using a Two-Phase Model: Theoretical Answer to the Phenomenon of Enhanced Heat Transfer

P. G. Siddheshwar[1]
Professor
Department of Mathematics,
Bangalore University,
Bangalore 560056, India
e-mail: pgsiddheshwar@bub.ernet.in

C. Kanchana
Department of Mathematics,
Bangalore University,
Bangalore 560056, India
e-mail: kanchanac@bub.ernet.in

Y. Kakimoto
Associate Professor
Department of Mechanical Engineering,
Shizuoka University,
3-5-1 Johoku, Naka-Ku,
Hamamatsu 432-8561, Japan
e-Email: tykakim@ipc.shizuoka.ac.jp

A. Nakayama
Professor
Department of Mechanical Engineering,
Shizuoka University,
3-5-1 Johoku, Naka-Ku,
Hamamatsu 432-8561, Japan;
School of Civil Engineering and Architecture,
Wuhan Polytechnic University,
Wuhan 430023, China
e-mail: tmanaka@ipc.shizuoka.ac.jp

Rayleigh–Bénard convection in liquids with nanoparticles is studied in the paper considering a two-phase model for nanoliquids with thermophysical properties determined from phenomenological laws and mixture theory. In the absence of nanoparticle-modified thermophysical properties as used in the paper, the problem is essentially binary liquid convection with Soret effect. The base liquids chosen for investigation are water, ethylene glycol, engine oil, and glycerine, and the nanoparticles chosen are copper, copper oxide, silver, alumina, and titania. Using data on these 20 nanoliquids, our theoretical model clearly explains advanced onset of convection in nanoliquids in comparison with that in the base liquid without nanoparticles. The paper sets to rest the tentativeness regarding the boundary condition to be chosen in the study of Rayleigh–Bénard convection in nanoliquids. The effect of thermophoresis is to destabilize the system and so is the effect of other parameters arising due to nanoparticles. However, Brownian motion effect does not have a say on onset of convection. In the case of nonlinear theory, the five-mode Lorenz model is derived under the assumptions of Boussinesq approximation and small-scale convective motions, and using it enhancement of heat transport due to the presence of nanoparticles is clearly explained for steady-state motions. Subcritical motion is shown to be possible in all 20 nanoliquids.
[DOI: 10.1115/1.4034484]

Keywords: nanoliquid, two-phase model, Rayleigh–Bénard convection

1 Introduction

Nanoliquid comprises of a base liquid such as water or ethylene-glycol or engine oil or glycerine with dilute concentration of nanoparticles such as metallic or metallic oxide particles (Cu, Cuo, Ag, Al_2O_3, TiO_2), having dimensions from 10 to 100 nm. It was Choi and Eastman [1] who first proposed the term "Nanoliquid." A significant feature of the nanoliquids is enhanced thermal conductivity, a phenomenon which was first reported by Masuda et al. [2]. Eastman et al. [3] reported an increase of 40% in the effective thermal conductivity of ethylene-glycol with 0.3 volume of copper nanoparticles of 10 nm diameter. Further, 10–30% increase of the effective thermal conductivity in alumina–water nanoliquids with 1–4% of alumina was reported by Das et al. [4]. Buongiorno [5] suggested a two-phase model based on the mechanics of nanoparticles/base liquid relative velocity. With the help of the transport equations of Buongiorno [5], Tzou [6,7] studied the onset of convection in a horizontal layer of a nanoliquid heated uniformly from below and found that as a result of Brownian motion and thermophoresis of nanoparticles, the critical Rayleigh number is much lower, by one to two orders of magnitude, than that of a base liquid. Kim et al. [8–10] investigated the onset of convection in a horizontal nanoliquid layer using a two-phase model and modified the three quantities, namely, the thermal expansion coefficient, the thermal diffusivity, and the kinematic diffusivity that appear in the definition of the Rayleigh number. Recently, many authors ([11–16] and references therein) have investigated various influences on Rayleigh–Bénard convection in nanoliquids. However, phenomenological laws and mixture theory do not seem to have been included in the study of Rayleigh–Bénard convection of nanoliquids.

The effect of Brownian motion was found to have negligible influence on both onset of convection and on heat and mass transports by previous investigators [1–16]. In view of the above observation, it is apparent that the handling of Rayleigh–Bénard convection in nanoliquids as reported by the earlier investigators has essentially been like a binary liquid system with the Soret effect. This is unacceptable since suspended nanoparticles are known to modify viscosity, thermal conductivity, and other thermophysical properties.

Classical two-phase models do not get explicitly into the modeling of nanoliquid properties like density, heat capacity, volumetric expansion coefficient, dynamic viscosity, thermal conductivity, Brownian, and thermophoretic coefficients in terms of the volume fraction of the nanoparticles and corresponding properties of nanoparticles and base liquid. Yang et al. [17] were the first to give details of such an exercise for forced convection. The new model mooted in this paper for studying Rayleigh–Bénard

[1]Corresponding author.

Contributed by the Heat Transfer Division of ASME for publication in the Journal of Heat Transfer. Manuscript received May 8, 2015; final manuscript received August 6, 2016; published online September 13, 2016. Assoc. Editor: Andrey Kuznetsov.

convection in nanoliquids incorporates such features with the help of phenomenological laws and mixture theory. As a result of these assumptions, thermodynamically correct predictions are sought to be made on the onset of convection and heat and mass transports for each nanoliquid under consideration.

The objectives of the present paper is the following:

(i) Provide a theoretical answer to the enhanced heat transfer situation in nanoliquids by combining features of the single-phase and two-phase models and
(ii) Settle the issue pertaining to the choice of appropriate Nield and Kuznetsov (NK) boundary condition [15,16] by using arguments on the magnitude of Sherwood number which has to be finite.

2 Mathematical Formulation for Rayleigh–Bénard Convection (Longitudinal Rolls)

Consider an infinite extent horizontal nanoliquid layer of thickness h. The upper and lower boundaries are held at constant temperatures T_0 and $T_0 + \Delta T(\Delta T > 0)$, respectively. The schematic of the same is shown in Fig. 1.

For mathematical tractability, we confine ourselves to two-dimensional rolls so that all the physical quantities are independent of y, a horizontal co-ordinate. Further, the boundaries are assumed to be stress-free and isothermal. The governing system of equations in dimensional form for studying stationary two-dimensional Rayleigh–Bénard convection in nanoliquids using a two-phase model are as follows.

Conservation of Mass:

$$\frac{\partial u}{\partial x} + \frac{\partial w}{\partial z} = 0 \tag{1}$$

Conservation of Linear Momentum:

$$\rho_{\rm nl}\left[\frac{\partial u}{\partial t} + u\frac{\partial u}{\partial x} + w\frac{\partial u}{\partial z}\right] = -\frac{\partial p}{\partial x} + \mu_{\rm nl}\nabla^2 u \tag{2}$$

$$\rho_{\rm nl}\left[\frac{\partial w}{\partial t} + u\frac{\partial w}{\partial x} + w\frac{\partial w}{\partial z}\right] = -\frac{\partial p}{\partial z} + \mu_{\rm nl}\nabla^2 w - \left[\rho_{\rm nl} - (\rho\beta)_{\rm nl}(T - T_0) + (\rho\beta)_\phi(\phi - \phi_0)\right]g \tag{3}$$

Conservation of Energy:

$$(\rho C_p)_{\rm nl}\left[\frac{\partial T}{\partial t} + u\frac{\partial T}{\partial x} + w\frac{\partial T}{\partial z}\right] = k_{\rm nl}\nabla^2 T + (\rho C_p)_{\rm np}\left[D_B\nabla\phi + \frac{D_T}{T_0}\nabla T\right]\cdot\nabla T \tag{4}$$

$$\frac{\partial \phi}{\partial t} + u\frac{\partial \phi}{\partial x} + w\frac{\partial \phi}{\partial z} = D_B\nabla^2\phi + \frac{D_T}{T_0}\nabla^2 T \tag{5}$$

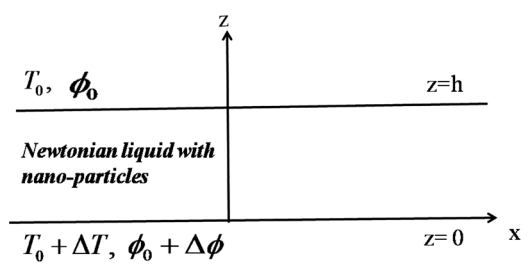

Fig. 1 Physical configuration

where

$$\nabla^2 = \frac{\partial^2}{\partial x^2} + \frac{\partial^2}{\partial z^2}, \quad D_B = \frac{(k_{B0}T)}{3\pi\mu_{\rm bl}d_{\rm np}}, \quad D_T = 0.26\frac{k_{\rm bl}}{2k_{\rm bl} + k_{\rm np}}\frac{\mu_{\rm bl}}{\rho_{\rm bl}}\chi$$

Assuming that the temperature and volumetric fraction of the nanoparticles to be constant at the stress-free boundaries, we may assume the boundary conditions on u, w, T, and ϕ to be

$$\left.\begin{aligned} &u = 0, \quad w = 0, \quad \frac{\partial u}{\partial z} + \frac{\partial w}{\partial x} = 0, \quad T = T_0 + \Delta T, \\ &\phi = \phi_0 + \Delta\phi \ \text{ at } \ z = 0 \\ &u = 0, \quad w = 0, \quad \frac{\partial u}{\partial z} + \frac{\partial w}{\partial x} = 0, \quad T = T_0, \\ &\phi = \phi_0 \ \text{ at } \ z = h \end{aligned}\right\} \tag{6}$$

Basic State Solution:

At the basic state the nanoliquid is assumed to be at rest, and hence, the temperature and nanoparticle volume fraction vary in the z-direction only and are given by

$$u = w = 0, \quad T = T_b(z), \quad \phi = \phi_b(z), \quad p = p_b(z) \tag{7}$$

Equations (2) and (3) now take the form

$$\frac{\partial p_b}{\partial x} = 0 \tag{8}$$

$$\frac{\partial p_b}{\partial z} + \left[\rho_{\rm nl} - (\rho\beta)_{\rm nl}(T_b - T_0) + (\rho\beta)_\phi(\phi_b - \phi_0)\right]g = 0 \tag{9}$$

Equation (4) using Eq. (7) now reads as

$$k_{\rm nl}\left(\frac{d^2T_b}{dz^2}\right) + (\rho c)_{\rm np}\frac{dT_b}{dz}\left[D_B\frac{d\phi_b}{dz} + \frac{D_T}{T_0}\frac{dT_b}{dz}\right] = 0 \tag{10}$$

Using an order of magnitude analysis, Nield and Kuznetsov [15] showed that the second and third terms in Eq. (10) are very small and hence from Eqs. (5), (7), and (10), we have

$$\frac{d^2T_b}{dz^2} = 0, \ \frac{d^2\phi_b}{dz^2} = 0 \tag{11}$$

The solution of Eq. (11) satisfying boundary conditions (6) is

$$T_b(z) = \left(1 - \frac{z}{h}\right)\Delta T + T_0, \quad \phi_b(z) = \left(1 - \frac{z}{h}\right)\Delta\phi + \phi_0 \tag{12}$$

Perturbation Solution:

We now superimpose perturbations on the basic state as shown below.

$$u = u', \quad w = w', \quad p = p_b + p', \quad T = T_b + T', \quad \phi = \phi_b + \phi' \tag{13}$$

Substituting the expression (13), using basic state solution (12), eliminating pressure, and introducing stream function of the form

$$u = -\frac{\partial \psi}{\partial z}, \quad w = \frac{\partial \psi}{\partial x} \tag{14}$$

the governing Eqs. (2)–(5) take the form

$$\rho_{\rm nl}\left[\frac{\partial}{\partial t}\left(\nabla^2\psi\right) + J\left(\psi, \nabla^2\psi\right)\right] = \mu_{\rm nl}\nabla^2\psi + (\rho\beta)_{\rm nl}g\frac{\partial T'}{\partial x} - (\rho\beta)_\phi g\frac{\partial \phi'}{\partial x} \tag{15}$$

$$(\rho C_p)_{nl}\left[\frac{\partial T'}{\partial t}+\frac{\partial \psi}{\partial x}\frac{\partial T'}{\partial z}-\frac{\partial \psi}{\partial z}\frac{\partial T'}{\partial x}+\frac{\partial \psi}{\partial x}\frac{dT_b}{dz}\right]$$
$$=k_{nl}\nabla^2 T'+(\rho C_p)_{np}D_B\left(\frac{\partial \phi'}{\partial x}\frac{\partial T'}{\partial x}+\frac{d\phi_b}{dz}\frac{\partial T'}{\partial z}+\frac{\partial \phi'}{\partial z}\frac{dT_b}{dz}+\frac{\partial \phi'}{\partial z}\frac{\partial T'}{\partial z}\right)$$
$$+(\rho C_p)_{np}\frac{D_T}{T_c}\left[\left(\frac{\partial T'}{\partial x}\right)^2+\left(\frac{\partial T'}{\partial z}\right)^2+2\cdot\frac{dT_b}{dz}\cdot\frac{\partial T'}{\partial z}\right] \quad (16)$$

$$\frac{\partial \phi'}{\partial t}+\frac{\partial \psi}{\partial x}\frac{\partial \phi'}{\partial z}-\frac{\partial \psi}{\partial z}\frac{\partial \phi'}{\partial x}=D_B\nabla^2\phi'+\frac{D_T}{T_c}\nabla^2 T'+\frac{\partial \psi}{\partial x}\frac{d\phi_b}{dz} \quad (17)$$

Introducing the following nondimensional variables

$$\left.\begin{aligned}(X,Z)&=\left(\frac{x}{h},\frac{z}{h}\right),\quad \tau=\frac{\alpha_{bl}t}{h^2},\quad \Psi=\frac{\psi}{\alpha_{bl}}\\ \Theta&=\frac{T'}{\Delta T},\quad \Phi=\frac{\phi'}{\Delta\phi}\end{aligned}\right\} \quad (18)$$

Equations (15)–(17) can be written in nondimensional form as

$$\frac{1}{\mathrm{Pr}_{nl}}\frac{\partial}{\partial\tau}(\nabla^2\Psi)$$
$$=a_1\nabla^4\Psi+R_{nl}a_1^2\frac{\partial\Theta}{\partial X}-R_{\phi_{nl}}a_1^2\frac{\partial\Phi}{\partial X}-\frac{1}{\mathrm{Pr}_{nl}}J(\Psi,\nabla^2\Psi) \quad (19)$$

$$\frac{\partial\Theta}{\partial\tau}=a_1\nabla^2\Theta+\frac{a_1N_{B_{nl}}}{\mathrm{Le}_{nl}}\left(\frac{\partial\Phi}{\partial X}\frac{\partial\Theta}{\partial X}-\frac{\partial\Theta}{\partial Z}-\frac{\partial\Phi}{\partial Z}+\frac{\partial\Phi}{\partial Z}\frac{\partial\Theta}{\partial Z}\right)$$
$$+\frac{a_1N_{A_{nl}}N_{B_{nl}}}{\mathrm{Le}_{nl}}\left[\left(\frac{\partial\Theta}{\partial X}\right)^2+\left(\frac{\partial\Theta}{\partial Z}\right)^2-2\frac{\partial\Theta}{\partial Z}\right]$$
$$+\frac{\partial\Psi}{\partial X}-J(\Psi,\Theta) \quad (20)$$

$$\frac{\partial\Phi}{\partial\tau}=\frac{a_1}{\mathrm{Le}_{nl}}\nabla^2\Phi+\frac{a_1N_{A_{nl}}}{\mathrm{Le}_{nl}}\nabla^2\Theta+\frac{\partial\Psi}{\partial X}-J(\Psi,\Phi) \quad (21)$$

where

$$a_1=\frac{\left[1-\frac{3\chi\left(1-\frac{k_{np}}{k_{bl}}\right)}{\left(\frac{k_{np}}{k_{bl}}+2\right)+\chi\left(1-\frac{k_{np}}{k_{bl}}\right)}\right]}{(1-\chi)+\chi\frac{(\rho C_p)_{np}}{(\rho C_p)_{bl}}}$$

$$R_{nl}=\frac{(\rho\beta)_{nl}\Delta T h^3 g}{\mu_{nl}\alpha_{nl}},\quad R_{\phi_{nl}}=\frac{(\rho_{np}-\rho_{nl})\Delta\phi h^3 g}{\mu_{nl}\alpha_{nl}}$$
$$N_{A_{nl}}=\frac{D_T\Delta T}{D_B T_c\Delta\phi},\quad N_{B_{nl}}=\frac{(\rho c)_{np}\Delta\phi}{(\rho c)_{nl}}$$
$$\mathrm{Pr}_{nl}=\frac{\mu_{nl}}{\rho_{nl}\alpha_E},\quad \mathrm{Le}_{nl}=\frac{\alpha_{nl}}{D_B}$$

The nanoliquid properties are obtained from either phenomenological laws or mixture theory as given below.
Phenomenological Laws:

$$\frac{\mu_{nl}}{\mu_{bl}}=\frac{1}{(1-\chi)^{2.5}},\quad \frac{k_{nl}}{k_{bl}}=\frac{\left(\frac{k_{np}}{k_{bl}}+2\right)-2\chi\left(1-\frac{k_{np}}{k_{bl}}\right)}{\left(\frac{k_{np}}{k_{bl}}+2\right)+\chi\left(1-\frac{k_{np}}{k_{bl}}\right)}$$

Mixture Theory:

$$\alpha_{nl}=\frac{k_{nl}}{(\rho C_p)_{nl}},\quad \frac{(\rho C_p)_{nl}}{(\rho C_p)_{bl}}=(1-\chi)+\chi\frac{(\rho C_p)_{np}}{(\rho C_p)_{bl}}$$
$$\frac{\rho_{nl}}{\rho_{bl}}=(1-\chi)+\chi\frac{\rho_{np}}{\rho_{bl}},\quad \frac{(\rho\beta)_{nl}}{(\rho\beta)_{bl}}=(1-\chi)+\chi\frac{(\rho\beta)_{np}}{(\rho\beta)_{bl}}$$

Equations (19)–(21) are solved subject to the isothermal, isoconcentration boundary conditions

$$\Psi=\frac{\partial^2}{\partial Z^2}\left(\frac{\partial\Psi}{\partial X}\right)=\Theta=\Phi=0\ \text{at}\ Z=0,1 \quad (22)$$

In Sec. 3, we discuss the linear stability analysis in order to predict the condition for the onset of convection.

3 Linear Stability Analysis

Before, when we perform a linear stability analyses we note that the principle of exchange stabilities is valid in the problem. Hence, we consider the linear, steady state of Eqs. (19)–(21) with the boundary condition (22) and assume the Fourier expansions for the normal mode as follows:

$$\Psi=A_{11}\sin(\pi\kappa X)\sin(\pi Z) \quad (23)$$

$$\Theta=B_{11}\cos(\pi\kappa X)\sin(\pi Z) \quad (24)$$

$$\Phi=C_{11}\cos(\pi\kappa X)\sin(\pi Z) \quad (25)$$

where A_{11}, B_{11}, and C_{11} are steady, infinitesimal amplitudes of the stream function, temperature, and concentration, respectively. Substituting Eqs. (23)–(25) in Eqs. (19)–(21) and taking the orthogonality condition with the eigenfunctions we get

$$\begin{bmatrix}\delta^4 & -\pi\kappa a_1 R^s_{nl_c} & \pi\kappa a_1 R_{\phi_{nl}}\\ \pi\kappa & -\delta^2 a_1 & 0\\ \pi\kappa & \frac{-a_1\delta^2 N_{A_{nl}}}{\mathrm{Le}_{nl}} & -\frac{a_1\delta^2}{\mathrm{Le}_{nl}}\end{bmatrix}\begin{bmatrix}A_{11}\\ B_{11}\\ C_{11}\end{bmatrix}=\begin{bmatrix}0\\0\\0\end{bmatrix}$$

The critical value of Rayleigh number, $R^s_{nl_c}$, and wave number, κ_c, are

$$R^s_{nl_c}=\frac{\delta^6}{\pi^2\kappa_c^2}+R_{\phi_{nl}}\mathrm{Le}_{nl}\left(1-\frac{N_{A_{nl}}}{\mathrm{Le}_{nl}}\right),\quad \kappa_c=\frac{1}{\sqrt{2}} \quad (26)$$

where $\delta^2=\pi^2(1+\kappa_c^2)$. The linear theory predicts only the condition for the onset of convection. To study the heat transport we move on to make a local nonlinear stability analysis of the system.

4 Nonlinear Stability Analysis

In the paper, we perform a weakly nonlinear stability analysis and hence take the stream function, temperature, and nanoparticle concentration as follows:

$$\Psi=\frac{\sqrt{2}a_1\delta^2}{\pi^2\kappa}A(\tau)\sin(\pi\kappa X)\sin(\pi Z) \quad (27)$$

$$\Theta=\frac{\sqrt{2}}{\pi r_{nl}}B(\tau)\cos(\pi\kappa X)\sin(\pi Z)-\frac{1}{\pi r_{nl}}C(\tau)\sin(2\pi Z) \quad (28)$$

$$\Phi=\frac{\sqrt{2}}{\pi}L(\tau)\cos(\pi\kappa X)\sin(\pi Z)+\frac{1}{\pi}M(\tau)\sin(2\pi Z) \quad (29)$$

where the amplitudes $A(\tau), B(\tau), C(\tau), L(\tau)$, and $M(\tau)$ are to be determined. Substituting Eqs. (27)–(29) in Eqs. (19)–(21) and taking the orthogonality condition with the eigenfunctions associated with the considered minimal modes, we get

$$\dot{A} = a_1 \mathrm{Pr}_{\mathrm{nl}}(B - A - r_{\phi_{\mathrm{nl}}} L) \tag{30}$$

$$\dot{B} = a_1 (r_{\mathrm{nl}} A - B - AC) \tag{31}$$

$$\dot{C} = a_1 (AB - bC) \tag{32}$$

$$\dot{L} = a_1 \left(A - \frac{N_{A_{\mathrm{nl}}}}{r_{\mathrm{nl}} \mathrm{Le}_{\mathrm{nl}}} B - \frac{1}{\mathrm{Le}_{\mathrm{nl}}} L + AM \right) \tag{33}$$

$$\dot{M} = a_1 \left(\frac{b N_{A_{\mathrm{nl}}}}{r_{\mathrm{nl}} \mathrm{Le}_{\mathrm{nl}}} C - \frac{b}{\mathrm{Le}_{\mathrm{nl}}} M - AL \right) \tag{34}$$

where $\tau_1 = \delta^2 \tau$, $b = (4\pi^2/\delta^2)$, $r_{\mathrm{nl}} = (\pi^2 \kappa^2 R_{\mathrm{nl}}/\delta^6)$, $r_{\phi_{\mathrm{nl}}} = (\pi^2 \kappa^2 R_{\phi_{\mathrm{nl}}}/\delta^6)$ and overdot denotes τ_1—derivative. It is well known in the context of the classical Lorenz model that its trajectories remain within the confines of a sphere. In Sec. 5, we show that the trajectories of the generalized Lorenz model are indeed trapped within an ellipsoid in five-dimensional phase-space.

5 Trapping Region

The trajectories of the classical Lorenz model are known to remain within a finite volume. The nonlinear terms are responsible for keeping the trajectories confined. Following the procedure of Siddheshwar and Titus [18], we can easily show that the trapping region of the trajectories is given by

$$A^2 + B^2 + (C - r_{\mathrm{nl}} - \mathrm{Pr}_{\mathrm{nl}})^2 + \frac{L^2}{\left(\frac{1}{\mathrm{Pr}_{\mathrm{nl}} r_{\Phi_{\mathrm{nl}}}}\right)} + \frac{M^2}{\left(\frac{1}{\mathrm{Pr}_{\mathrm{nl}} r_{\Phi_{\mathrm{nl}}}}\right)} = (\sqrt{2})^2 \tag{35}$$

From the above equation, we note that the trapping region is an ellipsoid in five-dimensional phase-space. The Lorenz model of Eqs. (30)–(34) is intractable but in the steady state it does possess a solution. This solution is arrived at in Sec. 6.

6 Steady Finite-Amplitude Convection

The penta-modal Lorenz model in the steady state has the solution

$$A^2 = \frac{-W_2 + \sqrt{W_2^2 - 4W_1 W_3}}{2W_1} \tag{36}$$

$$B = \frac{b r_{\mathrm{nl}} A}{(b + A^2)}, \quad C = \frac{r_{\mathrm{nl}} A^2}{b + A^2} \tag{37}$$

$$L = \mathrm{Le}_{\mathrm{nl}} A \left[1 - \frac{b N_{A_{\mathrm{nl}}}}{\mathrm{Le}_{\mathrm{nl}}(b + A^2)} - \frac{\mathrm{Le}_{\mathrm{nl}} A^2}{b + A^2 \mathrm{Le}_{\mathrm{nl}}^2} \times \left\{ \mathrm{Le}_{\mathrm{nl}} - \frac{b N_{A_{\mathrm{nl}}}}{b + A^2} \left(1 + \frac{1}{\mathrm{Le}_{\mathrm{nl}}} \right) \right\} \right] \tag{38}$$

$$M = \frac{-\mathrm{Le}_{\mathrm{nl}} A^2}{b + \mathrm{Le}_{\mathrm{nl}}^2 A^2} \left[\mathrm{Le}_{\mathrm{nl}} - \frac{b N_{A_{\mathrm{nl}}}}{b + A^2} \left(1 + \frac{1}{\mathrm{Le}_{\mathrm{nl}}} \right) \right] \tag{39}$$

where

$$W_1 = \mathrm{Le}_{\mathrm{nl}}^2 \tag{40}$$

$$W_2 = b \Big[(\mathrm{Le}_{\mathrm{nl}}^2 + 1) - r_{\mathrm{nl}} \mathrm{Le}_{\mathrm{nl}}^2 + r_{\phi_E} \mathrm{Le}_{\mathrm{nl}} (1 - N_{A_{\mathrm{nl}}} \mathrm{Le}_{\mathrm{nl}}) + r_{\phi_{nl}} \mathrm{Le}_{\mathrm{nl}}^2 N_{A_{\mathrm{nl}}} \left(1 + \frac{1}{\mathrm{Le}_{\mathrm{nl}}} \right) \Big] \tag{41}$$

$$W_3 = b^2 \left[(1 - r_{\mathrm{nl}}) + r_{\phi_{\mathrm{nl}}} \mathrm{Le}_{\mathrm{nl}} \left(1 - \frac{N_{A_{\mathrm{nl}}}}{\mathrm{Le}_{\mathrm{nl}}} \right) \right] \tag{42}$$

Equating the discriminant in Eq. (36) to zero, we obtain an equation for the finite-amplitude Rayleigh number, R_{nl}^f, as a quadratic equation as follows:

$$\frac{b^2 \kappa_c^4 \pi^4 \mathrm{Le}_{\mathrm{nl}}^4}{\delta^{12}} \left(R_{\mathrm{nl}}^f \right)^2 + \frac{2 b \kappa_c^2 \pi^2 \mathrm{Le}_{\mathrm{nl}}^2}{\delta^6} (2b - Q_1) R_{\mathrm{nl}}^f + (Q_1^2 - 4\mathrm{Le}_{\mathrm{nl}}^2 Q_2) = 0 \tag{43}$$

Solving Eq. (43), we get

$$R_{\mathrm{nl}}^f = \frac{-Q_4 - \sqrt{Q_4^2 - 4Q_3 Q_5}}{2Q_3} \tag{44}$$

where

$$Q_1 = b \Big[(\mathrm{Le}_{\mathrm{nl}}^2 + 1) + r_{\phi_{\mathrm{nl}}} \mathrm{Le}_{\mathrm{nl}} (1 - N_{A_{\mathrm{nl}}} \mathrm{Le}_{\mathrm{nl}}) + r_{\phi_{\mathrm{nl}}} \mathrm{Le}_{\mathrm{nl}}^2 N_{A_{\mathrm{nl}}} \left(1 + \frac{1}{\mathrm{Le}_{\mathrm{nl}}} \right) \Big]$$

$$Q_2 = b^2 + r_{\phi_{nl}} \mathrm{Le}_{\mathrm{nl}} \left(1 - \frac{N_{A_{\mathrm{nl}}}}{\mathrm{Le}_{\mathrm{nl}}} \right) b^2$$

$$Q_3 = \frac{b^2 \kappa_c^4 \pi^4 \mathrm{Le}_{\mathrm{nl}}^4}{\delta^{12}},$$

$$Q_4 = \frac{2 b \kappa_c^2 \pi^2 \mathrm{Le}_{\mathrm{nl}}^2 (2b - Q_1)}{\delta^6}$$

$$Q_5 = Q_1^2 - 4\mathrm{Le}_{\mathrm{nl}}^2 Q_2$$

In Sec. 7, we move on to estimate the heat and nanoparticle concentration transports at the lower boundary in terms of the Nusselt number and Sherwood number for the stationary mode of convection in a nanoliquid within a wave length distance in the horizontal direction.

7 Heat and Nanoparticle Concentration Transports

The thermal Nusselt number, $\mathrm{Nu}(\tau_1)$, is defined as

$$\mathrm{Nu}(\tau_1) = \frac{\text{heat transport by (conduction + convection)}}{\text{heat transport by conduction}} = 1 + \frac{k_{\mathrm{nl}}}{k_{\mathrm{bl}}} \left[\frac{\int_0^{\frac{2}{\kappa_c}} \left(\frac{\partial \Theta}{\partial Z} \right) dX}{\int_0^{\frac{2}{\kappa_c}} \left(\frac{d\Theta_b}{dZ} \right) dX} \right]_{Z=0} \tag{45}$$

where $\Theta_b = ((T_b - T_0)/\Delta T)$. The ratio $(k_{\mathrm{nl}}/k_{\mathrm{bl}})$ appears in the definition of the Nusselt number (45) due to the fact that k_{nl} is not distinguishable from k_{bl} in the conduction state due to slow heat transfer between the phases.

Substituting Eqs. (12) and (28) in Eq. (45), we get

$$\mathrm{Nu}(\tau_1) = 1 + \left(\frac{k_{\mathrm{nl}}}{k_{\mathrm{bl}}} \right) \frac{2}{r_{\mathrm{nl}}} C \tag{46}$$

The nanoparticle concentration Sherwood number, $\mathrm{Sh}(\tau_1)$, is defined as

$$\mathrm{Sh}(\tau_1) = \frac{\text{mass transport by (molecular diffusion + advection)}}{\text{mass transport by molecular diffusion}} = 1 + \left[\frac{\int_0^{\frac{2}{\kappa_c}} \left(\frac{1}{\mathrm{Le_{nl}}}\frac{\partial \Phi}{\partial Z} + \frac{N_{A_{\mathrm{nl}}}}{Le_{\mathrm{nl}}}\frac{\partial \Theta}{\partial Z}\right) dX}{\int_0^{\frac{2}{\kappa_c}} \left(\frac{1}{\mathrm{Le_{nl}}}\frac{d\Phi_b}{dZ} + \frac{N_{A_{\mathrm{nl}}}}{\mathrm{Le_{nl}}}\frac{d\Theta_b}{dZ}\right) dX}\right]_{Z=0} \tag{47}$$

Substituting Eqs. (12) and (29) in Eq. (47), we get

$$\mathrm{Sh}(\tau_1) = 1 + 2\frac{\left(\frac{N_{A_{\mathrm{nl}}}}{r_{\mathrm{nl}}}C - M\right)}{1 + N_{A_{\mathrm{nl}}}} \tag{48}$$

Substituting Eq. (37) in Eqs. (46) and (48), Nusselt and Sherwood numbers in the case of steady, finite-amplitude convection are obtained as follows:

$$\mathrm{Nu}(\infty) = 1 + \left(\frac{k_{\mathrm{nl}}}{k_{\mathrm{bl}}}\right)\frac{2A^2}{b + A^2} \tag{49}$$

$$\mathrm{Sh}(\infty) = 1 + 2\frac{\left(\frac{N_{A_{\mathrm{nl}}}A^2}{b + A^2} - M\right)}{1 + N_{A_{\mathrm{nl}}}} \tag{50}$$

where A^2 and M are given by Eqs. (36) and (39). In Sec. 8, we discuss the results obtained from the linear and nonlinear stability analyses and draw some conclusion.

8 Results and Discussion

Rayleigh–Bénard convection in nanoliquids is studied in the paper using the Buongiorno [5] two-phase model. The purpose of the present paper is to provide a theoretical answer to the phenomenon of enhanced heat transfer by combining features of the single-phase and two-phase models. In pursuing this line of thought, we follow the work of Yang et al. [17]. In addition to explaining the enhanced heat transfer, we also seek to make an important decision on the appropriateness of one of the two NK [15,16] boundary conditions in studying Rayleigh–Bénard convection with the help of arguments based on the finiteness of the Sherwood number.

To interpret the results obtained in the context of the 20 nanoliquids chosen for investigation in the paper, we have calculated the thermophysical properties of nanoliquids using the corresponding values of base liquids and nanoparticles (see Tables 1 and 2) together with the phenomenological laws for dynamic viscosity and thermal conductivity and expressions for other physical quantities using mixture theory.

It is important to note here that the specific heat and thermal expansion coefficient have been calculated using the following definitions:

$$(\mathrm{C}_p)_{\mathrm{nl}} = \frac{(\rho \mathrm{C}_p)_{\mathrm{nl}}}{\rho_{\mathrm{nl}}}, \quad \beta_{\mathrm{nl}} = \frac{(\rho\beta)_{\mathrm{nl}}}{\rho_{\mathrm{nl}}}$$

Table 1 Thermophysical properties of four base liquids at 300 °K

Base liquids	μ_{bl}	ρ_{bl}	k_{bl}	$\beta_{\mathrm{b1}} \times 10^5$	$\mathrm{C}_{p_{\mathrm{bl}}}$
Water	0.00089	997	0.613	21	4179
Ethylene glycol	0.0157	1114.4	0.252	65	2415
Engine oil	0.486	884	0.144	70	1910
Glycerine	0.799	1259.9	0.286	48	2427

Table 2 Thermophysical properties of five nanoparticles at 300 °K

Nanoparticles	ρ_{np}	k_{np}	$\beta_{\mathrm{np}} \times 10^5$	$\mathrm{C}_{p_{\mathrm{np}}}$
Copper	8933	401	1.67	385
Copper oxide	6320	76.5	1.8	531.8
Silver	10500	429	1.89	235
Alumina	3970	40	0.85	765
Titania	4250	8.9538	0.9	686.2

This is a discernible change in the modeling of $(\mathrm{C}_p)_{\mathrm{nl}}$ and β_{nl} for nanoliquids as compared to what has been used so far by most investigators. Typical values of the thermophysical properties of nanoliquids are documented in Table 3 that are calculated using values of thermophysical quantities of base liquids and nanoparticles extracted from the works of Ghasemi and Aminosadati [19], Siddheshwar and Meenakshi [20], Bergman et al. [21], and the paper by Abu-Nada et al. [22].

In the paper, we toe the line that enhanced the heat transfer by natural convection in nanoliquids under laminar flow conditions is due to thermophoretic effect and Brownian motion coupled with modification in the base liquid properties due to the presence of suspended nanoparticles.

The definition of the nondimensional parameters used in the paper are based on nanoliquid properties rather than base liquid properties. In doing so, we arrive at the critical nanoliquid Rayleigh number exactly the same as what was obtained by Bhadauria and Agarwal [11] using purely base liquid properties.

It is quite clear from Table 3 that the presence of nanoparticles increases the value of R_{nl_c} (see Eq. (26)) since $(N_{A_{\mathrm{nl}}}/\mathrm{Le_{nl}})$ is less than 1 in magnitude. This result does not help us in properly explaining the enhanced heat transfer in nanoliquids. To make a comparison between the results on heat transfer in Newtonian liquids without nanoparticles and that with nanoparticles, comparison need to be made between critical Rayleigh numbers of nanoliquid and the base liquid.

The factor, F, that arises when base liquid Rayleigh number, R_{bl}, is written in terms of nanoliquid Rayleigh number, R_{nl}, as follows:

$$R_{\mathrm{bl}} = \frac{R_{\mathrm{nl}}}{F}, \quad F = \frac{(\rho\beta)_{\mathrm{nl}}}{(\rho\beta)_{\mathrm{bl}}}\left(\frac{\mu_{\mathrm{bl}}}{\mu_{\mathrm{nl}}}\right)\cdot\left(\frac{\alpha_{\mathrm{bl}}}{\alpha_{\mathrm{nl}}}\right) \tag{51}$$

In the absence of nanoparticles, the value of F is 1. Computation reveals that the value of F for all 20 nanoliquids considered is less than 1. This would mean that $R_{\mathrm{nl}_c} < R_{\mathrm{bl}_c}$. This explains why one can expect enhanced heat transfer in nanoliquids.

We now move on to the discussion on the steady, finite-amplitude Rayleigh number, R^f_{nl}. Figure 2 is plot of the nanoliquid Rayleigh numbers, R^s_{nl} and R^f_{nl}. This plot explicitly demonstrates the existence of subcritical motion in water–titania nanoliquid. This nanoliquid is chosen for illustration as a representative nanoliquid amongst 20 nanoliquids chosen for investigation in the paper.

Figures 3–6 document the amount of heat transport as quantified by the thermal Nusselt number. When the results in these figures are seen in conjunction with Figs. 7 and 8, we may conclude that the nanoliquid in which convective activity is deep into the cell transports maximum heat. Among the 20 nanoliquids, we find that the ethylene-glycol–silver transports maximum heat while water–titania transports least.

The stream line plots 7 and 8 clearly show that the convective activity gets deep into the center of the cell in the case of ethylene-glycol–silver nanoliquid compared to other nanoliquids. At the other extreme, we find that the convective activity is less

Table 3 Thermophysical properties of nanoliquids at 300°K

Nanoliquids with $\chi = 0.06$.	μ_{nl}	ρ_{nl}	k_{nl}	α_{nl}	$N_{A_{nl}}$	Le_{nl}	$R_{\phi_{nl}}$	$N_{A_{nl}}/\mathrm{Le}_{nl}$
Water–copper	0.00104	1473.25	0.72981	1.77001×10^{-7}	4.38914	70.22265	2.67720	0.06250
Water–copper oxide	0.00104	1316.47	0.72743	1.76625×10^{-7}	4.88430	70.07326	2.68291	0.06970
Water–silver	0.00104	1567.27	0.72985	1.79548×10^{-7}	4.12620	71.23292	2.63923	0.05793
Water–alumina	0.00104	1175.47	0.72483	1.76827×10^{-7}	5.43715	70.15341	2.67985	0.07750
Water–titania	0.00104	1192.27	0.70808	1.73047×10^{-7}	5.16854	68.65375	2.73838	0.07528
Ethylene glycol–copper	0.01833	1583.52	0.30016	1.09701×10^{-7}	4.56756	68.37827	2.74941	0.06680
Ethylene glycol–copper oxide	0.01833	1426.74	0.29975	1.09741×10^{-7}	5.05754	68.40320	2.74841	0.07394
Ethylene glycol–silver	0.01833	1677.54	0.30017	1.12092×10^{-7}	4.31172	69.86861	2.69076	0.06171
Ethylene glycol–alumina	0.01833	1285.74	0.29930	1.1036×10^{-7}	5.59755	68.78903	2.73299	0.08137
Ethylene glycol–titania	0.01833	1302.54	0.29617	1.095×10^{-7}	5.42971	68.25298	2.75445	0.07955
Engine oil–copper	0.56731	1366.94	0.17154	9.56477×10^{-7}	4.16938	65.45580	2.87217	0.06370
Engine oil–copper oxide	0.56731	1210.16	0.17141	9.58242×10^{-7}	4.70324	65.57659	2.86688	0.07172
Engine oil–silver	0.56731	1460.96	0.17155	9.88627×10^{-7}	3.90113	67.65596	2.77876	0.05766
Engine oil–alumina	0.56731	1069.16	0.17126	9.67923×10^{-7}	5.31560	66.23910	2.83820	0.08025
Engine oil–titania	0.56731	1085.96	0.17021	9.65927×10^{-7}	5.17972	66.10251	2.84407	0.07836
Glycerine–copper	0.93267	1720.29	0.34064	1.10574×10^{-7}	4.75300	68.99905	2.72467	0.06888
Glycerine–copper oxide	0.93267	1563.51	0.34012	1.10573×10^{-7}	5.21567	68.99842	2.72470	0.07559
Glycerine–silver	0.93267	1814.31	0.34065	1.1271×10^{-7}	4.50689	70.33193	2.67304	0.06408
Glycerine–alumina	0.93267	1422.51	0.33954	1.11085×10^{-7}	5.71579	69.31792	2.71214	0.08246
Glycerine–titania	0.93267	1439.31	0.33555	1.10041×10^{-7}	5.53983	68.66645	2.73787	0.08068

into the center of the cell in the case of water–titania. This has an important bearing on the amount of heat transfer by these liquids.

The main emphasis in the paper is on heat transport aided by the nanoparticles. Since we have dilute concentration of nanoparticles in the base liquid, the quantification of mass transport in terms of the Sherwood number is not an important issue. We have, however, used the requirement of finiteness of the Sherwood number in settling questions regarding appropriate NK boundary condition on Φ (Nield and Kuznetsov [15,16]). If we were to choose the NK [16] boundary condition, then expression (47) clearly shows that the Sherwood number becomes infinite, whereas this is not so when we use the NK [15] boundary

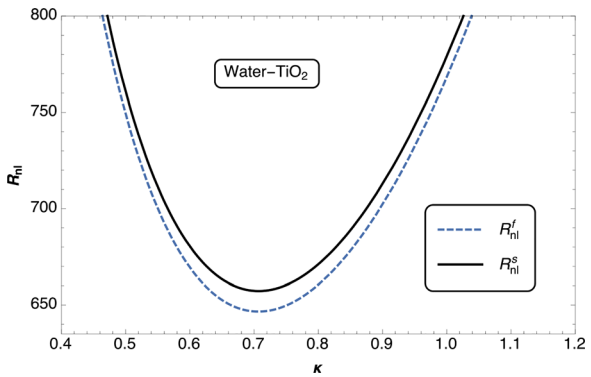

Fig. 2 Variation of thermal Rayleigh number, R_{nl}, with wave number, κ, for water–titania nanoliquid

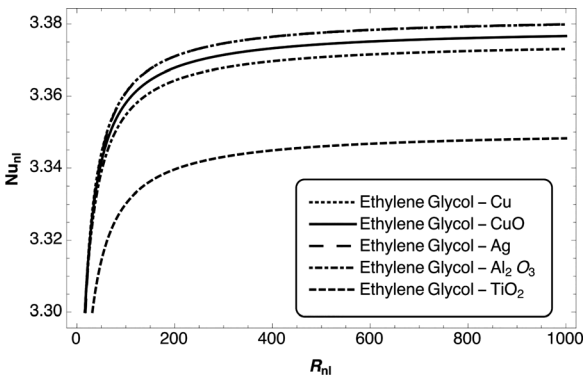

Fig. 4 Variation of Nu_{nl} with R_{nl} for ethylene glycol-based nanoliquids

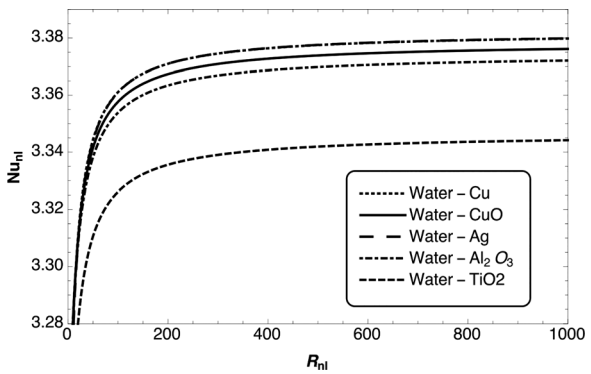

Fig. 3 Variation of thermal Nusselt number, Nu_{nl}, with thermal Rayleigh number, R_{nl}, for water-based nanoliquids

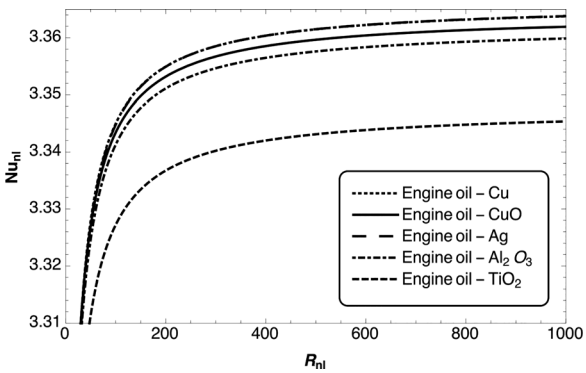

Fig. 5 Variation of Nu_{nl} with R_{nl} for engine oil-based nanoliquids

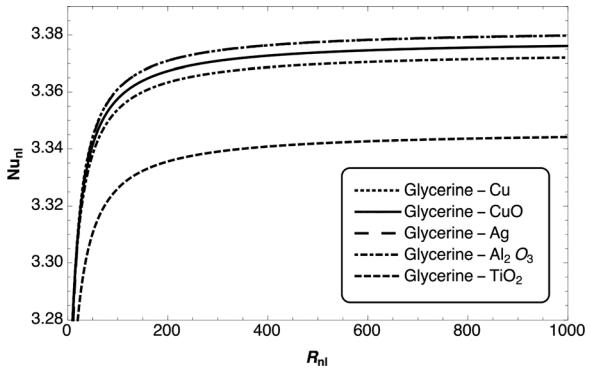

Fig. 6 Variation of $\mathrm{Nu_{nl}}$ with R_{nl} for glycerine-based nanoliquids

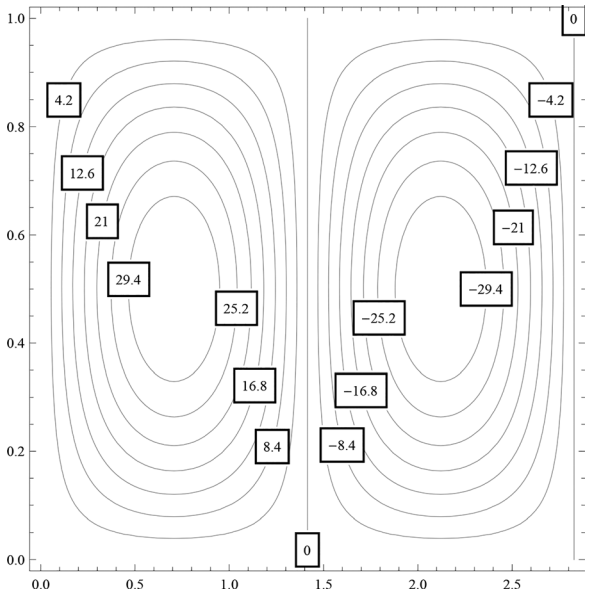

Fig. 7 Contour plot of stream function for ethylene-glycol–silver nanoliquid

condition. So we infer that the NK [15] boundary condition is the correct one for a study like ours.

9 Conclusion

(a) $R^s_{\mathrm{nl}_c}$ and $R^f_{\mathrm{nl}_c}$ are independent of $N_{B_{\mathrm{nl}}}$. $\mathrm{Nu_{nl}}$ is also independent of $N_{B_{\mathrm{nl}}}$. This means that only the thermophoretic effect has an influence on the onset of convection and on heat transport. This also means that in the absence of nanoparticle-modified thermophysical properties, the problem is that of binary liquid convection with Soret effect.

(b) $R^s_{\mathrm{nl}_c} < R^s_{\mathrm{bl}_c}$, $\mathrm{Nu_{nl}} > \mathrm{Nu_{bl}}$.

(c) $\frac{dR^s_{\mathrm{nl}_c}}{dR_{\phi_{\mathrm{nl}}}} < 0$, $\frac{dR^s_{\mathrm{nl}_c}}{d\mathrm{Le}_{\mathrm{nl}}} < 0$, $\frac{dR^s_{\mathrm{nl}_c}}{dN_{A_{\mathrm{nl}}}} < 0$.

(d) Subcritical instabilities are possible in all 20 nanoliquids.

(e) $\frac{dR^s_{\mathrm{nl}_c}}{d\chi} < 0$, $\frac{d\mathrm{Nu_{nl}}}{d\chi} > 0$.

(f) NK [15] boundary condition is the correct one to study Rayleigh–Bénard convection in nanoliquids.

(g) Computations reveal that qualitatively the results concerning 10% nanoparticles are similar to 6% particles, and hence, we have used only 6% in the paper.

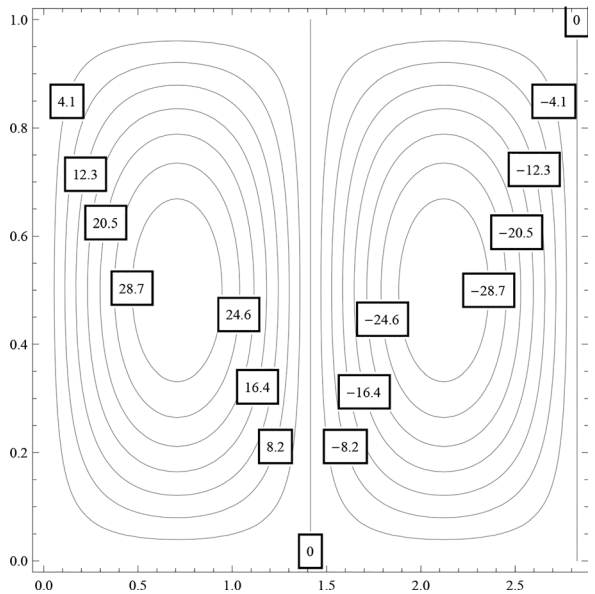

Fig. 8 Contour plot of stream function for water–titania nanoliquid

(h) Most of the reported studies use the Brinkman model for viscosity of nanoliquids and the Hamilton–Crosser model for thermal conductivity. The range of temperatures arising in the convective regime are slightly above the value corresponding to the critical temperature at onset and at best can result in marginal changes in the above two thermophysical quantities. The other thermophysical quantities are based on the mixture theory. Thermodynamically correct results have been obtained using the above models for thermophysical properties.

(i) In the absence of a reported accurate experiment to study convection in nanoliquids, it remains to be seen whether the single-phase [23] or the two-phase model [5] is appropriate.

(j) Corcione [24] has made comments of practical interest on the modeling of thermophysical quantities of nanoliquids, and a refined model based on these comments is warranted.

Nomenclature

A, B, C, L, M = amplitudes (m)
c = heat capacity (J/kg K)
d = diameter (m)
D = diffusion coefficient ($\mathrm{m^2/s}$)
$\mathbf{g}$ = acceleration due to gravity, $(0, 0, -g)$ $(\mathrm{m/s^2})$
h = dimensional liquid layer depth (m)
k = thermal conductivity (W/m K)
k_{B_0} = Boltzmann constant (J/K)
Le = Lewis number
N_A = modified diffusivity ratio
N_B = modified particle density increment
Nu = Nusselt number
p = dimensional dynamic pressure (Pa)
Pr = Prandtl number
R = Rayleigh number
Sh = Sherwood number
t = dimensional time (s)
T = dimensional temperature (K)
u = dimensional horizontal velocity (m/s)
w = dimensional vertical velocity (m/s)
x = dimensional horizontal coordinate (m)
X = nondimensional horizontal coordinate

z = dimensional vertical coordinate (m)
Z = nondimensional vertical coordinate

Greek Symbols

α = thermal diffusivity (m^2/s)
β = coefficient of thermal expansion (1/K)
Δ = difference in two values
Θ = nondimensional temperature
μ = dynamic coefficient of viscosity (kg/m s)
ν = kinematic viscosity (m^2/s)
ρ = density (kg/m^3)
κ = wave number (1/m)
τ = nondimensional time
ϕ = dimensional concentration of nanoparticles
Φ = nondimensional concentration of nanoparticles
χ = nondimensional nanoparticle volume fraction
ψ = dimensional stream function
Ψ = nondimensional stream function

Subscripts and Superscripts

b = basic state
bl = base liquid
B = Brownian
c = critical
f = finite-amplitude
nl = nanoliquid
np = nanoparticle
p = pressure
s = stationary
T = thermophoretic
$'$ = perturbed state
ϕ = concentration
0 = reference value

References

[1] Choi, S., and Eastman, J. A., 1995, "Enhancing Thermal Conductivity of Fluids With Nanoparticles," Int. Mech. Eng. Congr. Exh., Vol. 231, Paper No. W-31109-ENG-38.
[2] Masuda, H., Ebata, A., Teramae, K., and Hishinuma, N., 1993, "Alteration of Thermal Conductivity and Viscosity of Liquid by Dispersing Ultra Fine Particles," Netsu Bussei, **7**(4), pp. 227–233.
[3] Eastman, J. A., Choi, S. U. S., Li, S., Yu, W., and Thompson, L. J., 2001, "Anomalously Increased Effective Thermal Conductivities of Ethylene Glycol-Based Nanofluids Containing Copper Nanoparticles," Appl. Phys. Lett., **78**(6), pp. 718–720.
[4] Das, S. K., Putra, N., Thiesen, P., and Roetzel, W., 2003, "Temperature Dependence of Thermal Conductivity Enhancement for Nanofluids," ASME J. Heat Transfer, **125**(4), pp. 567–574.
[5] Buongiorno, J., 2006, "Convective Transport in Nanofluids," ASME J. Heat Trans., **128**(3), pp. 240–250.
[6] Tzou, D. Y., 2008, "Instability of Nanofluids in Natural Convection," ASME J. Heat Transfer, **130**(7), p. 072401.
[7] Tzou, D. Y., 2008, "Thermal Instability of Nanofluids in Natural Convection," Int. J. Heat Mass Trans., **51**(11–12), pp. 2967–2979.
[8] Kim, J., Kang, Y. T., and Choi, C. K., 2004, "Analysis of Convective Instability and Heat Transfer Characteristics of Nanofluids," Phys. Fluids, **16**(7), pp. 2395–2401.
[9] Kim, J., Choi, C. K., Kang, Y. T., and Kim, M. G., 2006, "Effects of Thermodiffusion and Nanoparticles on Convective Instabilities in Binary Nanofluids," Nanoscale Microscale Thermophys. Eng., **10**(1), pp. 29–39.
[10] Kim, J., Kang, Y. T., and Choi, C. K., 2007, "Analysis of Convective Instability and Heat Transfer Characteristics of Nanofluids," Int. J. Refrig., **30**(2), pp. 323–328.
[11] Bhadauria, B. S., and Agarwal, S., 2014, "Convective Heat Transport by Longitudinal Rolls in Dilute Nanoliquids," J. Nanofluids, **3**(4), pp. 380–390.
[12] Dhananjaya, Y., Agarwal, G. S., and Bhargava, R., 2011, "Rayleigh–Bénard Convection in Nanofluid," Int. J. Appl. Math. Mech., **7**(2), pp. 61–76.
[13] Dhananjaya, Y., Agarwal, G. S., and Bhargava, R., 2011, "Thermal Instability of Rotating Nanofluid Layer," Int. J. Eng. Sci., **49**(11), pp. 1171–1184.
[14] Jawdat, J. M., Hashim, I., and Momani, S., 2012, "Dynamical System Analysis of Thermal Convection in a Horizontal Layer of Nanofluids Heated From Below," Corp., Math. Prob. Eng., **2012**, pp. 1–13.
[15] Nield, D. A., and Kuznetsov, A. V., 2009, "Thermal Instability in a Porous Medium Layer Saturated by a Nanofluid," Int. J. Heat Mass Trans., **52**(25–26), pp. 5796–5801.
[16] Nield, D. A., and Kuznetsov, A. V., 2014, "Thermal Instability in a Porous Medium Layer Saturated by a Nanofluid: A Revised Model," Int. J. Heat Mass Trans., **68**, pp. 211–214.
[17] Yang, C., Sano, Y., Li, W., Mochizuki, M., and Nakayama, A., 2013, "On the Anomalous Convective Heat Transfer Enhancement in Nanofluids: A Theoretical Answer to the Nanofluids Controversy," ASME J. Heat Transfer, **135**(5), p. 054504.
[18] Siddheshwar, P. G., and Titus, P. S., 2013, "Nonlinear Rayleigh–Bénard Convection With Variable Heat Source," ASME J. Heat Transfer, **135**(12), p. 122502.
[19] Ghasemi, B., and Aminossadati, S. M., 2009, "Natural Convection Heat Transfer in an Inclined Enclosure Filled With a Water—CuO Nanofluid," Numer. Heat Transfer, **55**(8), pp. 807–823.
[20] Siddheshwar, P. G., and Meenakshi, N., 2016, "Amplitude Equation and Heat Transport for Rayleigh–Benard Convection in Newtonian Liquids With Nanoparticles," Int. J. Appl. Comput. Math., **2**, pp. 1–22.
[21] Bergman, T. L., Lavine, A. S., Incropera, F. P., and Dewitt, D. P., 2006, *Fundamentals of Heat and Mass Transfer*, Wiley, New York.
[22] Abu-Nada, E., Masoud, Z., and Hijazi, A., 2008, "Natural Convection Heat Transfer Enhancement in Horizontal Concentric Annuli Using Nanofluids," Int. Commun. Heat Mass Transfer, **35**(5), pp. 657–665.
[23] Khanafer, K., Vafai, K., and Lightstone, M., 2003, "Buoyancy-Driven Heat Transfer Enhancement in a Two-Dimensional Enclosure Utilizing Nanofluids," Int. J. Heat Mass Trans., **46**(19), pp. 3639–3653.
[24] Corcione, M., 2011, "Rayleigh–Bénard Convection Heat Transfer in Nanoparticle Suspensions," Int. J. Heat Fluid Flow, **32**(1), pp. 65–77.